Metadata of the article that will be visualized in OnlineFirst

ArticleTitle	Characterizing and modelling the coupled in-plane shear-biaxial tension deformation response of unidirectional non-crimp fabrics
Article Sub-Title	
Article CopyRight	
Journal Name	International Journal of Material Forming

Corresponding Author	FamilyName	**Montesano**
	Particle	
	Given Name	**John**
	Suffix	
	Division	Composites Research Group, Department of Mechanical & Mechatronics Engineering
	Organization	University of Waterloo
	Address	200 University Ave. West, Waterloo, ON, N2L 3G1, Canada
	Phone	
	Fax	
	Email	john.montesano@uwaterloo.ca
	URL	
	ORCID	
Corresponding Author	FamilyName	**Ghazimoradi**
	Particle	
	Given Name	**Mehdi**
	Suffix	
	Division	Composites Research Group, Department of Mechanical & Mechatronics Engineering
	Organization	University of Waterloo
	Address	200 University Ave. West, Waterloo, ON, N2L 3G1, Canada
	Phone	
	Fax	
	Email	mehdi.ghazimoradi@uwaterloo.ca
	URL	
	ORCID	http://orcid.org/0000-0002-7875-8087
Author	FamilyName	**Carvelli**
	Particle	
	Given Name	**Valter**
	Suffix	
	Division	Department A.B.C
	Organization	Politecnico di Milano
	Address	Piazza Leonardo Da Vinci 32, Milan, 20133, Italy
	Phone	
	Fax	
	Email	
	URL	
	ORCID	

Schedule	Received	9 Sep 2022
	Revised	
	Accepted	2 May 2023

Abstract	The coupled biaxial tension and shear-biaxial tension deformation responses of a unidirectional non-crimp fabric (UD-NCF) was explored using a novel experimental test setup. A custom multiaxial loading system was used to subject multibranched fabric specimens to combined in-plane tension loads. Biaxial tension tests conducted with varying ratios of deformation along the orthogonal carbon fiber tow and supporting glass fiber yarn directions revealed minor tension-tension deformation coupling over the deformation range considered. Combined shear-equibiaxial tension tests were also conducted with different deformation rates along the fabric diagonal direction, where variations in the force-strain response revealed notable shear-extension coupling. A macroscopic finite element simulation model was developed for the fabric, which employed an available constitutive model that captured the anisotropic hyperelastic response of the fibers. The simulation model accurately predicted the fabric coupled shear-extension deformation for the combined shear-equibiaxial test cases and revealed that the shear angle at the specimen center was limited by the applied tension along the orthogonal fibers. The simulation model was also used to predict shear angle contours for multibranched specimens with different fiber orientations. It was demonstrated that the extent of shear deformation is sensitive to the direction of tension loads. These important findings provide an improved understanding of the coupled deformation modes for UD-NCFs, which will aid in future studies focused on their formability.
Keywords (separated by '-')	Unidirectional non-crimp fabric - Coupled shear-biaxial tension deformation - Multi-directional experimental testing - Macroscopic simulation model
Footnote Information	

International Journal of Material Forming _####################_
https://doi.org/10.1007/s12289-023-01757-0

ORIGINAL RESEARCH

Characterizing and modelling the coupled in-plane shear-biaxial tension deformation response of unidirectional non-crimp fabrics

John Montesano[1] · Mehdi Ghazimoradi[1] · Valter Carvelli[2]

Received: 9 September 2022 / Accepted: 2 May 2023

Abstract

The coupled biaxial tension and shear-biaxial tension deformation responses of a unidirectional non-crimp fabric (UD-NCF) was explored using a novel experimental test setup. A custom multiaxial loading system was used to subject multibranched fabric specimens to combined in-plane tension loads. Biaxial tension tests conducted with varying ratios of deformation along the orthogonal carbon fiber tow and supporting glass fiber yarn directions revealed minor tension-tension deformation coupling over the deformation range considered. Combined shear-equibiaxial tension tests were also conducted with different deformation rates along the fabric diagonal direction, where variations in the force-strain response revealed notable shear-extension coupling. A macroscopic finite element simulation model was developed for the fabric, which employed an available constitutive model that captured the anisotropic hyperelastic response of the fibers. The simulation model accurately predicted the fabric coupled shear-extension deformation for the combined shear-equibiaxial test cases and revealed that the shear angle at the specimen center was limited by the applied tension along the orthogonal fibers. The simulation model was also used to predict shear angle contours for multibranched specimens with different fiber orientations. It was demonstrated that the extent of shear deformation is sensitive to the direction of tension loads. These important findings provide an improved understanding of the coupled deformation modes for UD-NCFs, which will aid in future studies focused on their formability.

Keywords Unidirectional non-crimp fabric · Coupled shear-biaxial tension deformation · Multi-directional experimental testing · Macroscopic simulation model

Introduction

During the last decade, unidirectional non-crimp fabrics (UD-NCFs) have been widely applied in various industries such as aeronautic, automotive, and wind energy due to their good drapability characteristics and ease of handling during processing of liquid composite molded parts. The first step in liquid composite molding processes typically involves preforming of the dry fabric layers into a three-dimensional near-net shape. During preforming of UD-NCFs, the complex interactions between the fabric constituents (e.g., local tow-stitching yarn interaction) can result in undesirable defects such as tow gapping and wrinkling [1–3]. Forming processes can be optimized to reduce the severity of these defects by manipulating the inherently coupled macroscopic in-plane shear and tension deformation modes of the fabric. While several studies have focused on assessing the coupled tension-tension and shear-tension deformation response of woven and other multiaxial fabrics [4–10], few have studied these coupled responses for UD-NCFs [11]. An improved understanding of the coupled in-plane deformation response of reinforcement fabrics can support the development and calibration of robust macroscopic forming simulation models [12].

Several experimental tests have been developed and utilized to characterize the in-plane tension and shear deformation response of reinforcement fabrics. Uniaxial off-axis extension tests comprising specimens subjected to loading

✉ John Montesano
john.montesano@uwaterloo.ca

✉ Mehdi Ghazimoradi
mehdi.ghazimoradi@uwaterloo.ca

[1] Composites Research Group, Department of Mechanical & Mechatronics Engineering, University of Waterloo, 200 University Ave. West, Waterloo, ON N2L 3G1, Canada

[2] Department A.B.C, Politecnico di Milano, Piazza Leonardo Da Vinci 32, Milan 20133, Italy

Journal : Large 12289	Article No : 1757	Pages : 14	MS Code : 1757	Dispatch : 14-5-2023

along a single direction have been used to capture the shear response of several types of fabrics [5, 13, 14], including UD-NCFs [1, 3, 15–17]. Uniaxial extension tests have also been used to characterize the extension response of UD-NCFs along the primary fiber directions [1, 16, 18]. Picture frame tests involving specimens clamped in a fixture loaded along two dependent directions have been widely used to characterize the shear deformation response of reinforcement fabrics [4, 19], although in recent studies these tests have been deemed unsuitable for UD-NCFs [1, 16]. Biaxial extension tests have also been developed to capture the tension-tension coupling deformation response of various fabrics. Carvelli et al. [4] demonstrated that a biaxial tension test setup with a cruciform specimen was suitable to capture the coupled tension-tension response of a three-dimensional non-crimp woven fabric. Digital image correlation (DIC) was used to measure warp and weft direction normal strain contours at the center of the cruciform specimens. Ghazimoradi et al. [5] performed a similar study for a tetraxial fabric where a cruciform specimen was loaded in a custom biaxial test frame and DIC was used to measure normal strain fields and shear angle contours. In a recent study by the authors [11], a biaxial test frame was used to investigate the coupled tension-tension response of a UD-NCF. Test performed at different biaxial displacement ratios revealed the interdependency of the orthogonal tensile deformation modes of the fabric caused by the interactions between the carbon fiber tows, glass fiber yarns, and stitching segments. The center region of the cruciform specimens used in the study underwent slight inhomogeneous deformation due to the local fabric deformation modes, which was captured through DIC measured normal strains.

Few studies have focused on characterizing the in-plane shear-tension coupling of reinforcement fabrics. Many of the early investigations focused on capturing the coupled shear-tension response of fabrics by applying a pre-tension to a fabric test specimen along the principal fiber directions prior to placement within the shear test rig [6–9, 12]. Launay et al. [7] utilized a picture frame rig with controlled pre-tensioning for a woven fabric. Their results showed that the level of pre-tension has an influence on the shear rigidity of the fabric, especially during loading through low shear angles. Kashani et al. [10] used a biaxial picture frame test fixture to simultaneously load a woven fabric cruciform specimen under combined shear and tension loading. It was revealed that the in-plane shear stiffness of the woven fabric increased with the increasing pre-tension, while the tensile behavior of the fabric becomes more compliant when undergoing in-plane shear deformation. Harrison [20] used a biaxial bias extension test setup (Fig. 1) to study the coupled shear-tension response of fabrics, where a normalization theory was developed to extract the shear and tensile responses. Abdiwi et al. [9] and Potluri [21] utilized the

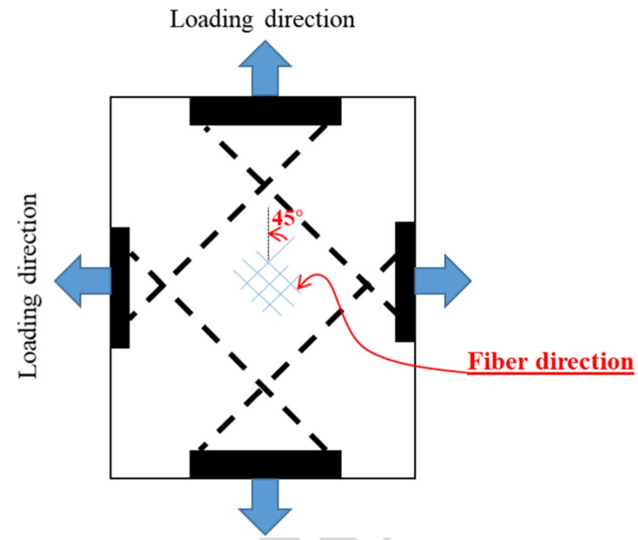

Fig. 1 Biaxial-shear specimen used in [20]

same approach to study mixed-mode deformation of woven and other biaxial fabrics. Using previously reported methods to characterize the shear-tension coupling of fabrics does not allow for the application of various displacement ratios along each loading direction simultaneously (i.e., multiple independent loading directions), which is a notable limitation. Moreover, an assessment of the coupled shear-tension response of UD-NCFs, which is the focus of the present study, has not been reported in the literature.

Finite element (FE)-based forming models are commonly developed using either a mesoscopic or macroscopic representation of the reinforcement fabric. Mesoscopic models capture the detailed fabric structure and the local interactions between the different constituents [22]. On the other hand, macroscopic models capture the effective mechanical behavior of reinforcement fabrics. These models treat the fabric as a homogeneous continuum with embedded local deformations, which requires the development of a customized material model for a specific fabric. Macroscopic forming simulation models provide a more computationally efficient means to simulate preforming processes for full scale complex shaped components. Several macroscopic forming simulation models have been developed for reinforcement fabrics utilizing either a hyperelastic or hypoelastic material model with the assumption of decoupled membrane deformation modes [22–29]. Schäfer et al. [30] developed a macroscopic forming model for woven fabrics that captures biaxial deformation coupling through a nonlinear hyperelastic material model. Their study revealed the importance of capturing this coupled deformation mode to accurately predict fabric deformation and defects during preforming. Other macroscopic forming models have been developed that also capture either the biaxial coupling or shear-tension

Journal : Large 12289	Article No : 1757	Pages : 14	MS Code : 1757	Dispatch : 14-5-2023

coupling of woven fabrics [31–34]. Constitutive models used for UD-NCFs typically assume that the in-plane deformation modes are uncoupled, despite experimental evidence revealing that such coupling exists [1, 16]. Schirmaier et al. [3] developed a comprehensive macroscopic forming model for UD-NCFs that considers coupling between in-plane tension and shear deformations. The material model consists of a non-orthogonal elastic-plastic material deformation response with a custom linear strain measure, where in-plane shear-tension coupling was captured. However, the model requires a significant number of material parameters to be calibrated using inverse approaches. Schäfer et al. [35] reported a simplified model for UD-NCF that neglects in-plane deformation mode coupling, revealing that although numerical predictions are reasonable there are limitations for forming simulations. They reported that use of a hyperelastic material model may improve prediction forming-induced wrinkling defects. Senner et al. [36] developed a semi-discrete FE simulation model to capture the membrane deformation response of UD-NCFs. The transversely isotropic hyperelastic membrane response was captured using continuum-based shell elements and the stitching segments were modelled using beam elements. Although the in-plane shear deformation response was captured for a simple picture frame test, the interactions between the stitching and the unidirectional tows was neglected which may not enable accurate simulation of coupled shear-tension response.

A review of the literature reveals a lack of experimental studies focused on investigating the coupled biaxial tension and shear-biaxial tension response of UD-NCFs, while few numerical models have been developed to adequately capture this response for UD-NCFs. In this paper, a novel experimental setup utilizing a new test specimen geometry is proposed to characterize the coupled shear-biaxial tension deformation response of a binder stabilized heavy-tow carbon fiber UD-NCF. Shear-biaxial tension coupling tests were performed by simultaneously loading the specimens along three independent directions with various deformation ratios, including the two principal orthogonal fabric directions and the diagonal direction. A macroscopic FE simulation model employing an available anisotropic hyperelastic constitutive model was developed to predict the coupled biaxial tension and shear-biaxial tension response of the UD-NCF. The simulation model also facilitated an additional study focused on capturing the effect of fiber orientation on the coupled shear-biaxial tension response of the fabric.

Material and test setup

Fabric features and test specimens

A commercially available UD-NCF, namely Zoltek™ PX35-UD300, was investigated. The heavy-tow fabric comprised 5 mm wide tows each containing 50,000 PX35 carbon fiber (CF) filaments. The parallel tows were stitched together with polyester yarn in a tricot pattern (Fig. 2). The supporting glass fiber (GF) yarns were

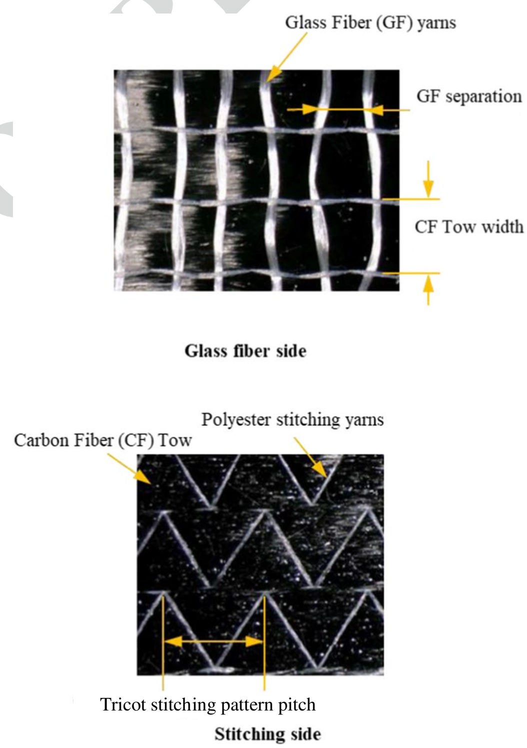

Parameter	Value (mm)
GF yarn separation	3.6±0.7
CF tow width	5
Stitching pattern pitch	7
Fabric thickness	0.49±0.02

Fig. 2 Images of Zoltek™ PX35-UD300 unidirectional non-crimp fabric showing architecture from both stitching and glass fiber yarn sides

oriented perpendicular to the CF tows and positioned between the CFs and the polyester stitching (Fig. 2). A light thermosetting binder powder was uniformly distributed on the stitching side of the fabric. The total fabric areal density was 333 g/m^2 with the carbon fiber tows accounting for 92.8% of the total weight.

All test specimens used in this study were cut from one roll of the UD-NCF fabric. The shear-biaxial tension specimens had six loading arms, each with a width of 100 mm (Fig. 3a). The biaxial tensile specimens were cruciform, comprising four loading arms (Fig. 3b). A pair of tabs were glued to the clamping zone of each arm for all specimens using 3 M-3430 epoxy adhesive.

Experimental test setup

A custom device equipped with 12 independent hinged jacks oriented along two orthogonal axes was used to perform all tests in this study (Fig. 3). The device comprised a planetary gearbox to transform rotational motion from the motors mounted on each jack into linear motion, where the maximum displacement rate and stroke of each jack were 240 mm/min and 512 mm, respectively. A 15 kN capacity load cell was mounted on each jack (see Ref [11] for further details).

First, biaxial tensile tests were performed using cruciform specimens (Fig. 3b) with different longitudinal (CF tow direction) to transverse (GF yarn direction) displacement rate ratios, R. The biaxial tensile tests included equibiaxial

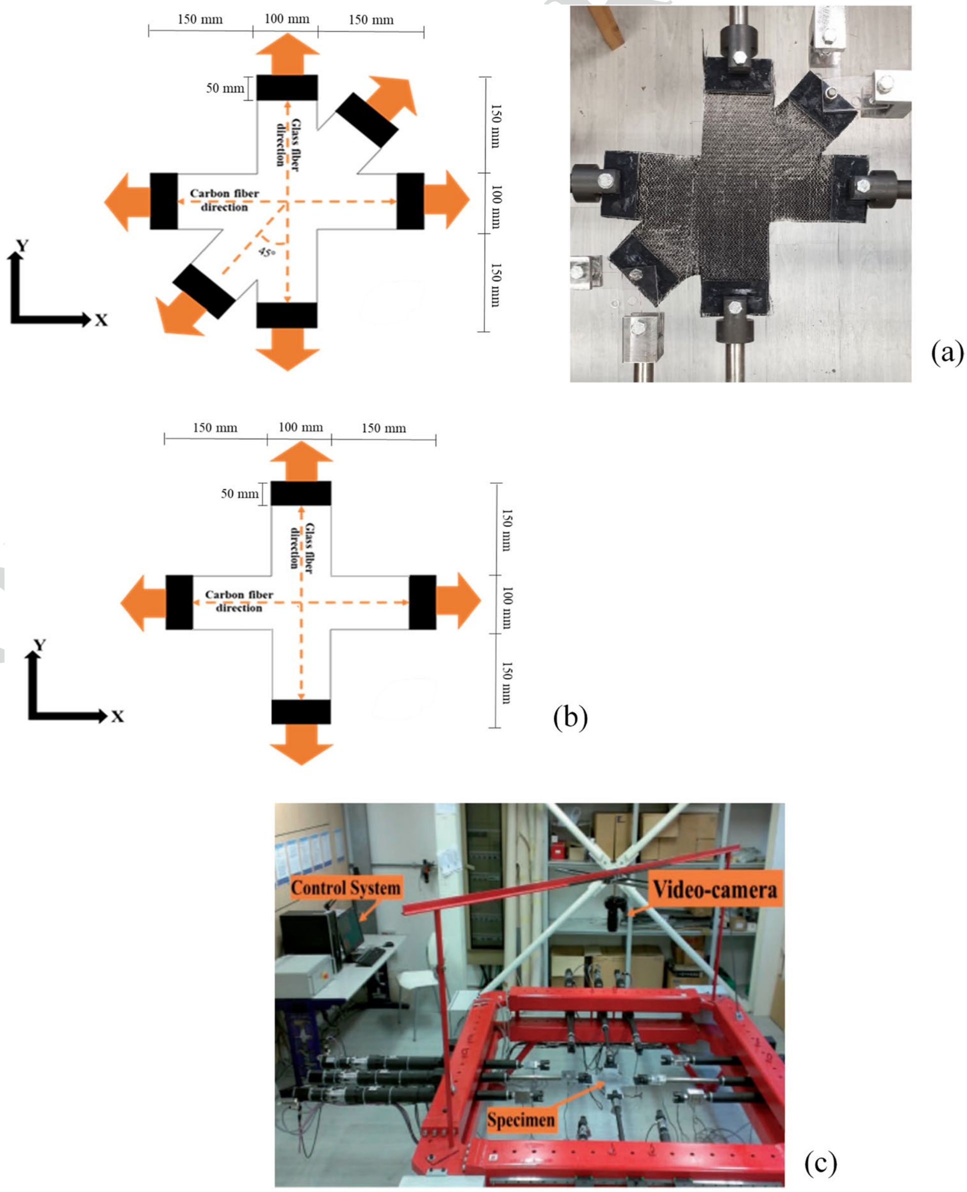

Fig. 3 Dimensions of the: **a** multiaxial in-plane specimen, and **b** biaxial tensile specimen (tabs shown in black). **c** multiaxial in-plane tensile device

Journal : Large 12289	Article No : 1757	Pages : 14	MS Code : 1757	Dispatch : 14-5-2023

(R = 1) where the transverse and longitudinal displacement rates were set to 1 mm/min, and disproportional where the longitudinal displacement rate was set to 0.5 mm/min (R = 0.5) or 2 mm/min (R = 2) with a transverse displacement rate of 1 mm/min. Further details of the biaxial tensile tests are provided in Ref [11], including details of the two-dimensional DIC setup used to estimate the strain field at the center of the cruciform specimen within a region of interest (ROI) measuring 50 × 50 mm^2. It should be noted that the strain measures reported in this study for the biaxial tests are logarithmic strain.

Mixed-mode (shear-biaxial tension) tests were also performed on multiaxial specimens (Fig. 3a) with various ratios of deformation along the three loading directions. For the first set of tests, specimens were subjected to an equibiaxial displacement rate of 1 mm/min along both the CF tow and GF yarn directions and a constant displacement rate of 2 mm/min along the diagonal direction (denoted as Sh2_B1). The second set of tests were similar to the first, except that the displacement rate along the diagonal was 8 mm/min (denoted as Sh8_B1). Note, DIC evaluations for the shear-biaxial tension tests are not presented due to image decorrelation issues that occurred when processing the captured images. Instead, the normal strains along the loading arms were determined from the corresponding displacements and, thus, represent engineering strains.

Computational simulation model overview

A macroscopic simulation model was developed in this study using the commercial FE software LS-DYNA® and the available material constitutive model *MAT_249 [37]. A new formulation of this material model for UD-NCFs was used considering three fiber families. This formulation enabled capture of the anisotropic extensional response of the fabric along the longitudinal, transverse, and diagonal directions, respectively representing extension of the CF tows, supporting GF yarns, and the stitching. Each fiber family was treated as a hyperelastic material with a user-defined preferential direction (i.e., 0°, 90°, and 45° directions) [38], where the extensional response of each is assumed to be uncoupled [37]. In recent work [1], it was shown that the extensional response of a UD-NCF along the longitudinal (CF tow) and transverse (GF yarn) directions are slightly coupled for low normal strains, which provides support for this assumption (discussed further in Coupled biaxial tension deformation section). In this study, the shear response between fiber families is assumed to be elasto-plastic. Note, the material model assumes that shear response is not directly coupled to the extensional deformation response along the axis of each fiber family. However, the use of a third fiber family representing the stitching enabled capture of the coupled in-plane shear-extension deformation response of the fabric as a result of the superposition of the stiffness along the stitching direction, which was calibrated along with the fabric in-plane shear response. Further details of the material model and the calibration process for the input parameters used are provided in [39]. For the sake of brevity, only the main parameters are described hereafter.

A brief description of the key input parameters of the material model for the studied UD-NCF are summarized in Table 1. For each fiber family, an input curve was used to specify stress as a function of the fiber strain (see LCEFi parameters in Table 1 and Ref. [37]), which enabled capture of their nonlinear extensional stress-strain response [1]. In previous work, it was shown that the in-plane shear response of the UD-NCF followed a characteristic three-stage profile [1]. In this study, the elasto-plastic shear response of the fiber families, representing the initial two-stages of fabric shear deformation, was captured using specified shear stress-shear angle data (see LCG12 parameter in Table 1 and Ref. [37]). The fabric in-plane shear locking angle (ALOC12) and the shear modulus for shear angles greater than the shear locking angle (GLOC12; third stage of fabric shear deformation) were set to 0.58 radians and 4.82 MPa, respectively. Note, the input data for the shear response between fiber families 2 and 3 were assumed to be the same as that between fiber families 1 and 2 for this study. Although not important for this study, the out-of-plane shear moduli corresponding to the first fiber family were set to G31_1 = 4.35 MPa and G23_1 = 3.15 MPa. Since the CF tows and GF yarns are orthogonal, the transverse shear moduli corresponding to the second fiber family are set to G31_2 = 3.15 MPa and G23_2 = 4.35 MPa.

Fully integrated shell finite elements (Type 16) with three integration points through the thickness were used to mesh the single layer multi-branch specimens in the macroscopic simulation models. The average element size used for the simulations was set to 5.0 mm as determined by a preliminary sensitivity analysis (results not shown). Boundary conditions were applied to the ends of the specimen branches to mimic the displacements applied in the experiments (i.e., for

Table 1 Key input parameters for material model *MAT_249 [37]

Variable	Description
LCEF1	CF tow extension stress-strain data
LCEF2	GF yarn extension stress-strain data
LCEF3	Stitching extension stress-strain data
G23_1	Transverse shear modulus perpendicular to CF tow
G31_1	Transverse shear modulus along CF tow
LCG12	In-plane shear stress-shear angle data
ALOC12	In-plane shear locking angle
GLOC12	In-plane shear linear modulus after shear locking

Journal : Large 12289 | Article No : 1757 | Pages : 14 | MS Code : 1757 | Dispatch : 14-5-2023

each specimen branch a defined in-plane displacement was applied along its axis). The out-of-plane displacement of the specimen was constrained in all simulations. For each loading case, an explicit simulation was performed and the large deformation option was chosen. Note, the strains reported for the simulation model predictions are taken as the average strain at the specimen center within a 50×50 mm^2 ROI.

Results and discussion

Coupled biaxial tension deformation

The results for all biaxial tension tests performed on the cruciform specimens with different displacement rate ratios, R, were previously reported in Ref. [11] and are briefly summarized in this section to provide a comparison with the results predicted using the numerical model. Experimental data included in the subsequent plots for each displacement rate ratio represents the average response from a set of at least three repeated tests. Note, the reported strain components were taken as the average at the center of the cruciform specimens within the 50×50 mm^2 ROI through DIC evaluations. The force-strain response along the CF tow (Fig. 4a) and GF yarn (Fig. 4b) directions for all biaxial tests performed at different displacement rate ratios was nonlinear. The tow-in response for both directions was due to the extension of initially slack fibers, where a stiffer response was observed after straightening of the fibers [1]. Measured forces along the CF tow direction were significantly larger than the GF yarn direction for all displacement ratios, owing to the higher reinforcement content and fabric stiffness along that direction. The force-strain response along the CF tow (longitudinal) direction for all R values was similar, with the apparent stiffness of the fabric increasing slightly for R = 0.5. This slightly coupled deformation response is due to the interactions between the stitching and the CF tows and GF yarns [11]. Variation in the force-strain response and apparent fabric stiffness along the GF yarn direction for different R values, particularly for R = 1, further reveals the coupled biaxial deformation response of the fabric (Fig. 4b). Experimental strain contours along the CF tow direction at the center of the specimens (Fig. 5a-c) reveal slight inhomogeneous deformation for all displacement ratios, which is a result of localized deformations of the stitching and CF tows. Nevertheless, the longitudinal normal strain field at the specimen center within the ROI was relatively uniform (similar for all repeated tests). The degree of inhomogeneous deformation was more pronounced along the transverse direction for all displacement ratios (Fig. 6a-c) due to minor tow gapping observed during the tests.

Predicted longitudinal force-strain responses for all displacement ratios (Fig. 4a) correlated well with the experimental data for the displacement range considered. However, the simulation model underpredicted the transverse force-strain response for R = 1 for strains exceeding 0.3% and overpredicted the response for R = 0.5 for strains exceeding 0.15% (Fig. 4b). This discrepancy may be a result of the assumed uncoupled extensional deformation response for each fiber family in the material model, which seems to be less accurate for larger deformations. Furthermore, the simulation model is unable to capture the local fabric deformations, which is a common characteristic for all macroscopic models. Nevertheless, the simulation model captured the coupled biaxial tension deformation response at lower normal strains, which is attributed to the use of three fiber families in the material model that enabled indirect coupling due to the superposition of the distinct stiffnesses for each fiber family. The fabric nonlinear tow-in response was also captured by the simulation model along both the CF and GF directions, owing to the use of tabulated uniaxial extensional stress-strain data for both directions as input [39]. The

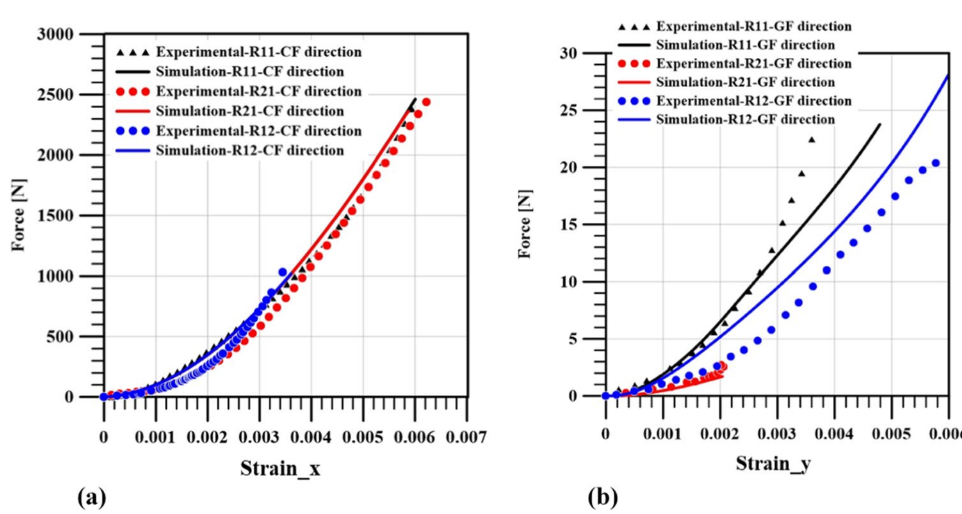

Fig. 4 Force-strain response for indicated biaxial tests along: **a** CF tow direction (x), and **b** GF yarn direction (y). Displacement rate ratios denoted R = 1 (R11), R = 2 (R21), and R = 0.5 (R12)

Journal : Large 12289 | Article No : 1757 | Pages : 14 | MS Code : 1757 | Dispatch : 14-5-2023

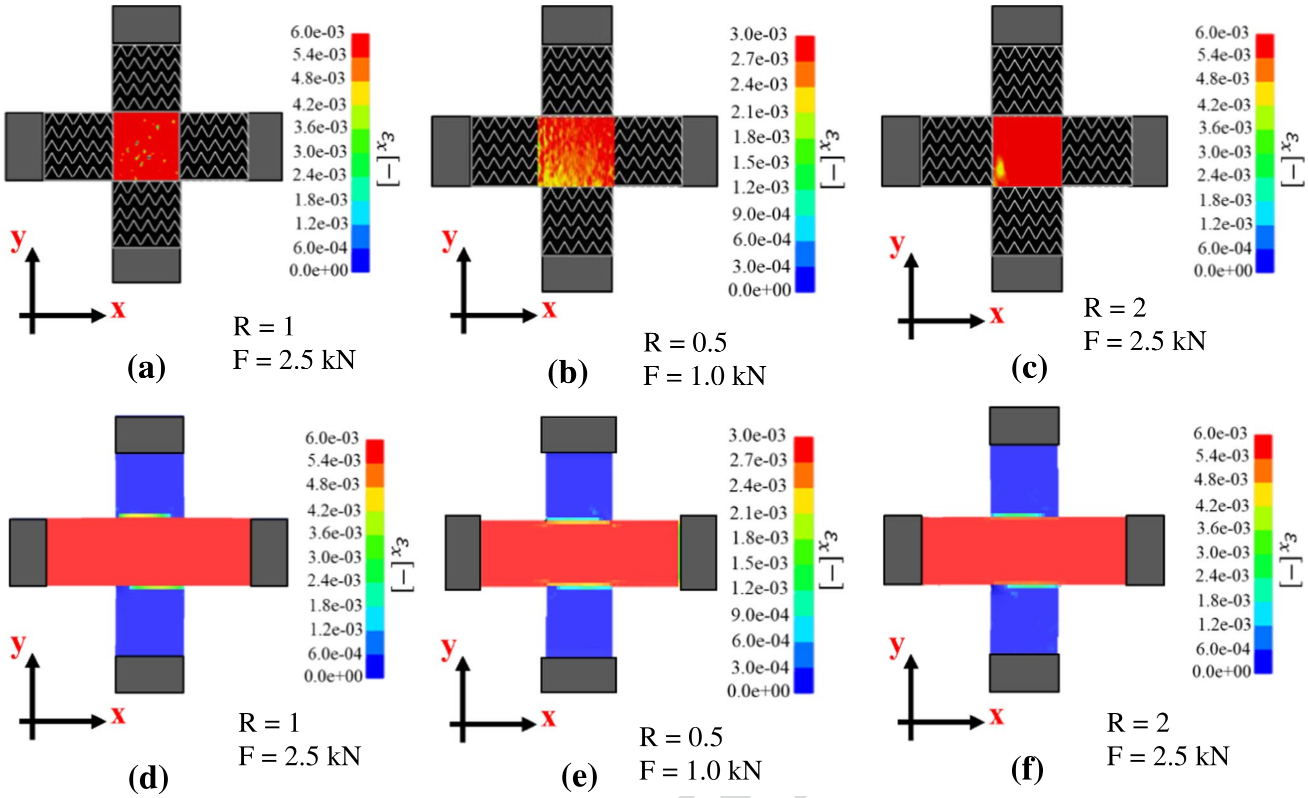

Fig. 5 Biaxial test longitudinal strain (ε_x) contours along CF tow direction: **a**-**c** experimental (DIC), and **d**-**e** predicted. Displacement rate ratios (R) and longitudinal force (F) are indicated

predicted strain contours along the CF direction at the center of the cruciform specimens were also uniform (Fig. 5d-f), with the average strain corresponding well to the experimental values for all R values. The simulation model predicted relatively uniform strains along the transverse direction (Fig. 6d-f). These results contrast with the inhomogeneous strain fields captured during the experiments, which is attributed to the inability of the macroscopic simulation model to capture local fabric deformations.

Coupled shear-biaxial tension deformation

Experimental data included in the subsequent plots for each shear-biaxial tension test represents the average response from a set of at least three repeated tests, where the repeatability was high with a scatter about the average < 10% (scatter not shown in Fig. 7 for better clarity). The force-strain response along the CF tow (Fig. 7a) and GF yarn (Fig. 7b) directions was nonlinear for all shear-biaxial tension tests, which included a similar tow-in response as was observed for biaxial tension tests (Coupled biaxial tension deformation section). Increasing the displacement rate along the diagonal specimen branch caused a slight increase in the apparent stiffness of the UD-NCF along the CF tow direction (compare Sh2_B1 and Sh8_B1 plots in Fig. 7a). This coupled shear-extension deformation response is attributed to the interactions between the stitching web and CF tows during the shear-biaxial tension tests, which was also reported to be observed during off-axis extension tests performed on the same UD-NCF [1]. Nevertheless, owing to the high stiffness of the fabric along the CF direction, the change in measured force along this direction of the multi-branched specimens with increasing diagonal displacement ratio is not pronounced (i.e., increase in force by 11% at an axial strain of 0.35%). Due to the lower fabric stiffness along the GF yarn direction, increasing the displacement rate along the diagonal branch had a more notable influence on the deformation response along this direction (i.e., 45% force increase at a transverse strain of 0.6%). The captured diagonal force-strain responses for the same shear-biaxial tension tests revealed a higher resistance to deformation along this direction during the initial stage of loading, followed by a slight reduction between 0.2 and 0.4% strain before increasing at higher strains (Fig. 7c). During the initial stage, deformation along the diagonal direction was inhibited due to the friction between the stitching segments and the CF tows, which was overcome during the second stage of loading. The apparent stiffness of the fabric increased along the diagonal direction with increasing diagonal displacement rate (compare Sh2_B1 and Sh8_B1 in Fig. 7c), which further

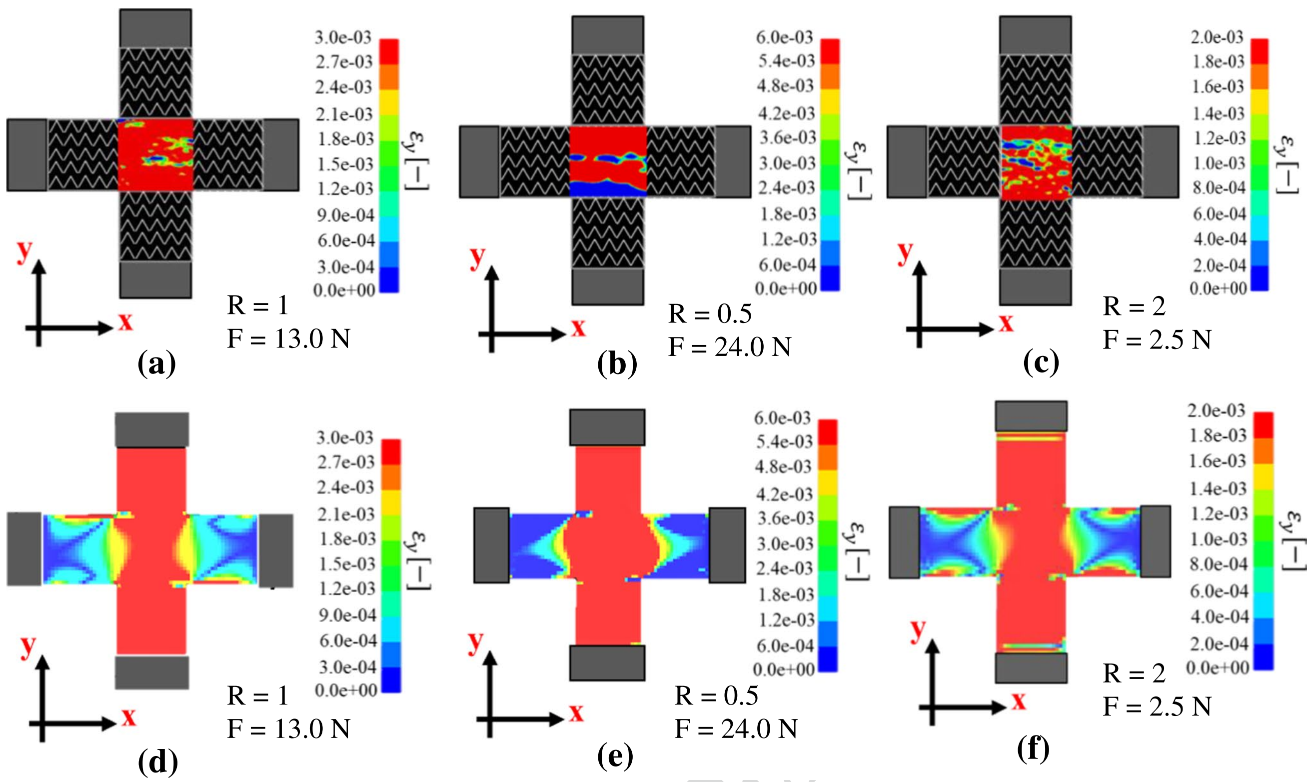

Fig. 6 Biaxial test transverse strain (ε_y) contours along GF yarn direction: **a-c** experimental (DIC), and **d-e** predicted. Displacement rate ratios (R) and transverse force (F) are indicated

demonstrates the coupled shear-extension deformation response of the UD-NCF. Note, due to the fiber orientation within the multi-branched specimens the extent of shear deformation at the specimen center was limited (will be discussed subsequently). It must also be noted that the diagonal displacement rate was 4× higher for the Sh8_B1 tests and rate effects may have also contributed to the increased fabric stiffness captured along the diagonal direction.

Predicted longitudinal force-strain responses for shear-biaxial tests for both displacement ratios (Fig. 7a) correlated well with the experimental data for the displacement range considered (< 10% deviation). The predicted force-strain response along the GF yarn direction for the Sh2_B1 tests tended to deviate from the experimentally obtained response at higher magnitudes of deformation (Figs. 7b and 22% deviation at a transverse strain of 0.5%). This discrepancy may be a result of the material model which assumes an uncoupled extensional deformation response along the CF tow and GF yarn directions. Nevertheless, the predicted multi-stage force-strain response along the diagonal direction for both Sh2_B1 and Sh8_B1 tests correlated very well with the experimental data (Fig. 7c), which demonstrates the capability of the simulation model to capture the coupled shear-extension deformation of the UD-NCF. The importance of capturing the coupled shear and extensional deformation in macroscopic simulation models for UD-NCFs was previously reported [35]. The predicted normal strain contours along the CF tow direction are similar for both the Sh2_B1 and Sh8_B1 tests for the same level of force, with a minor difference in the magnitude of strain at the specimen center (Fig. 8a-d). The predicted normal strain contours along the GF yarn direction are also similar for both the Sh2_B1 and Sh8_B1 tests, with a slightly greater discrepancy (Fig. 8e-h). For all predictions, the normal strain contours are nearly uniform within the 50×50 mm^2 ROI at the specimen center. The predicted shear angle contours for both shear-biaxial tension tests at the same diagonal displacement magnitude reveals that an increase in the diagonal displacement rate does not change the magnitude of the shear angle at the specimen center (Fig. 9a-b). This finding is due to the high stiffness of the fabric along the CF tow direction (horizontal branch of the specimen) and the fact that the biaxial extension deformation along the CF tow and GF yarn directions tends to suppress fabric shear deformation. This coupled shear-extension response has been previously reported for woven fabrics [10]. The predicted diagonal force for the Sh8_B1 test was 75% higher when compared to the Sh2_B1 test, which supports this point. The FE model was also used to simulate a test on the

Journal : **Large 12289**	Article No : **1757**	Pages : **14**	MS Code : **1757**	Dispatch : **14-5-2023**

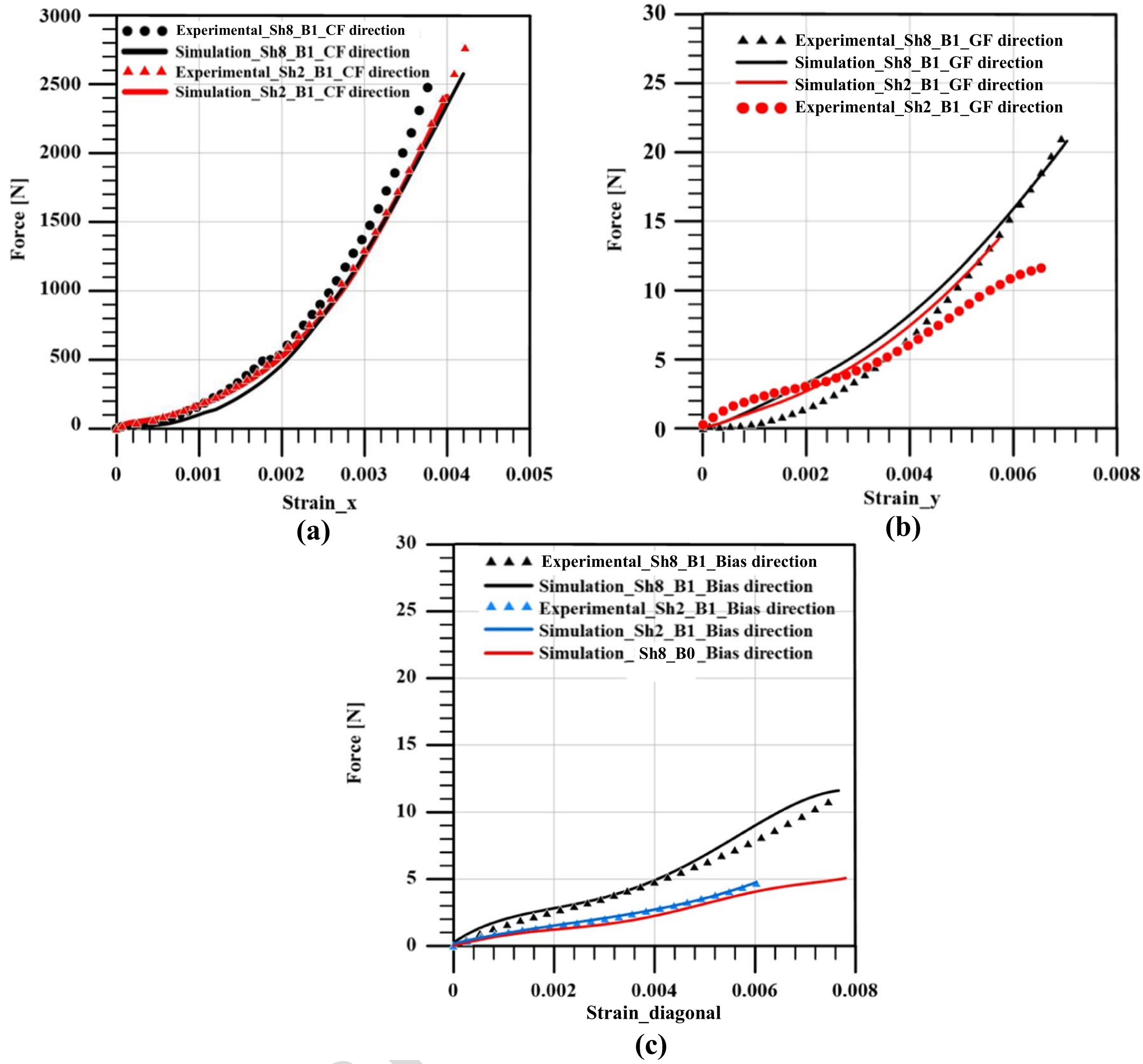

Fig. 7 Force-strain response for indicated shear-biaxial tension tests along: **a** CF tow direction (x), **b** GF yarn direction (y), and **c** diagonal direction. Note, the data in all plots comprises normal engineering strains

multi-branched specimen with displacement only applied to the diagonal branch, denoted as Sh8_B0, which was not experimentally considered. The force-shear response along the diagonal direction deviated from that of the Sh8_B1 test (Fig. 7c), while the associated shear angle contour reveals a higher degree of shear deformation with a 43% reduction in the magnitude of force along the diagonal direction (Fig. 9c). In other words, the tension along the perpendicular branches of the Sh8_B1 specimen tended to suppress shear deformation more than that observed for the Sh8_B0 specimen where there was no tension along these branches. This result further demonstrates the effect of tension along the CF tow and GF yarn directions on the shear deformation response of the UD-NCF. It should be noted that the superimposed tensions captured in the vertical and diagonal arms of the multi-branched specimens (Fig. 8) may have influencing the shear deformation at the specimen center and the observed shear-extension deformation coupling.

Effect of fiber orientation on coupled shear-biaxial tension deformation

In the previous section, the capability of the developed simulation model to capture the coupled shear-extension deformation response of the UD-NCF was demonstrated. In a subsequent study, the FE model was used to capture the shear angle contours at the center of the multi-branch specimens for cases when the CF tow orientation was biased at +45° or -45° from the horizontal branch, which enabled further assessment of the fabric coupled shear-extension deformation response. Three tests were simulated with a

Journal : **Large 12289**	Article No : **1757**	Pages : **14**	MS Code : **1757**	Dispatch : **14-5-2023**

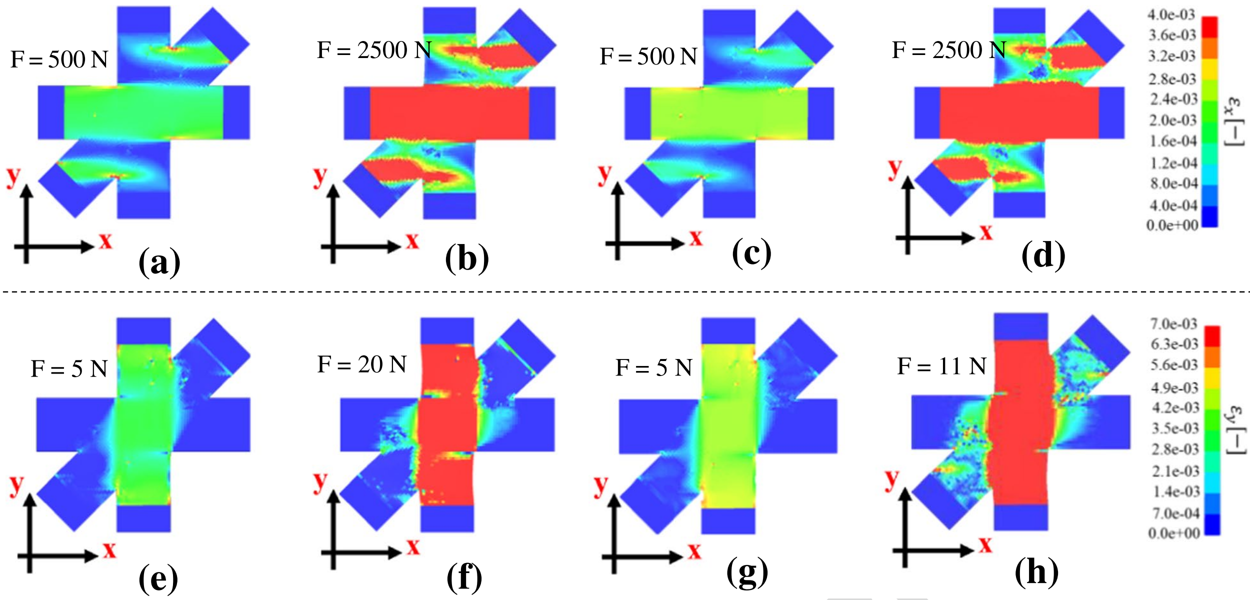

Fig. 8 Predicted strain component (ε_x) contour plot at indicated force along the CF tow direction (x): (**a**-**b**) Sh8_B1 test, (**c**-**d**) Sh2_B1 test. Predicted strain component (ε_y) contour plot at indicated force along the GF yarn direction (y): (**e**-**f**) Sh8_B1 test, (g-h) Sh2_B1 test

displacement rate of 1 mm/min along the diagonal branch and various equibiaxial displacement rates along the horizontal and vertical branches, including 2 mm/min (Sh1_B2), 8 mm/min (Sh1_B8), and 16 mm/min (Sh1_B16). The predicted shear angle contours captured at the same magnitude of displacement along the diagonal direction were distinct when compared to the case when the CF tows were aligned with the specimen horizontal branch, with an overall increase in the magnitude of shear angle at the specimen center (compare Figs. 9 and 10, see Table 2). This increase in shear angle is a direct result of the CF tow orientation and the fact that tension is only applied to either the CF tow direction or the GF yarn direction, which enabled increased shear deformation. It is also interesting that the magnitude of shear angle was larger for the tests with −45° CF tow orientation when compared to the tests with +45° CF tow orientation, for all considered biaxial displacement rates (Table 2). For the former tests the fabric was tensioned along the GF yarns (i.e., lower fiber content and stiffness direction) which enabled greater shear deformation. For the latter tests, the fabric was tensioned along the CF tow direction (i.e., stiffer direction), which led to relatively lower fabric shear deformation. This result further demonstrates that the coupled shear-extension deformation of the UD-NCF is sensitive to the direction of the tension loading. For both cases, the average shear angle at the specimen center increased with increasing displacement rate along the perpendicular branches (Table 2), with the −45° case showing greater sensitivity to the displacement rate as expected since the GF yarns are tensioned. It is interesting to note that the magnitude of shear angle increased linearly with increasing equibiaxial displacement for the +45° case, while the trend was nonlinear for the −45° case (Fig. 11).

Conclusions

The aim of this investigation was to evaluate the inherent coupled in-plane biaxial tension and shear-biaxial tension deformation responses of a unidirectional non-crimp

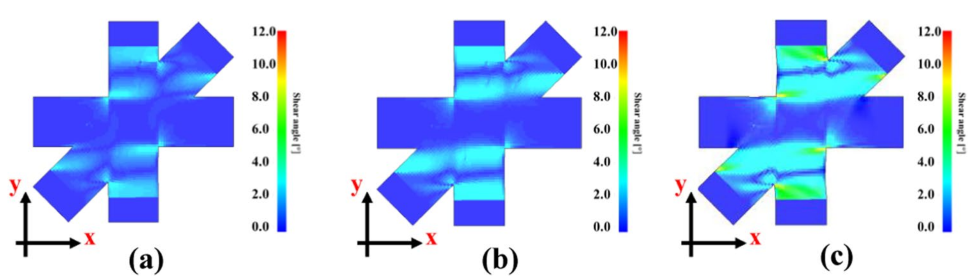

Fig. 9 Predicted shear angle contour plot captured at a diagonal displacement of 1 mm: **a** Sh2_B1 test, **b** Sh8_B1 test, and **c** Sh8_B0 test

Journal : **Large 12289** | Article No : **1757** | Pages : **14** | MS Code : **1757** | Dispatch : **14-5-2023**

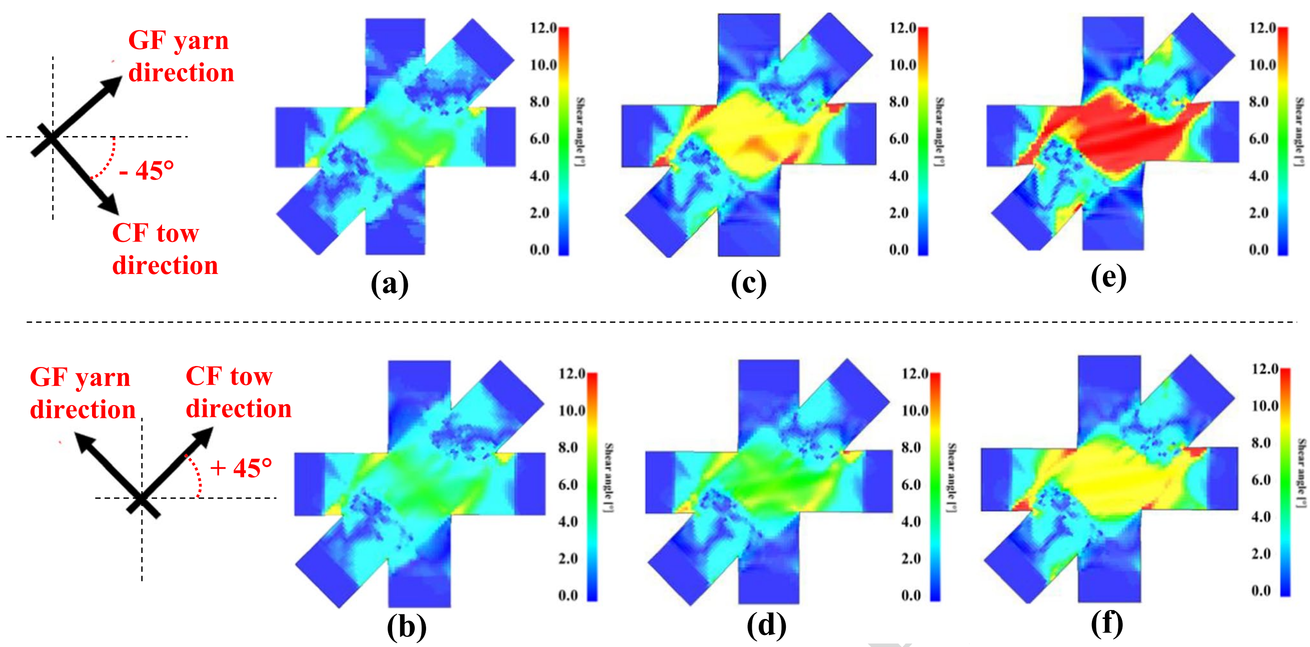

Fig. 10 Predicted shear angle contour plot captured at a diagonal displacement of 1 mm for indicated fiber orientation: **a-b** Sh1_B2 test, **c-d** Sh1_B8 test, and **e-f** Sh1_B16 test

fabric (UD-NCF). A novel experimental test setup comprising a custom multiaxial loading system and a digital image correlation (DIC) measurement system was used where multibranched fabric specimens were subjected to combined in-plane tension loads. A macroscopic finite element model was utilized to simulate the experimental tests and assess its feasibility in capturing the coupled membrane deformation modes of the fabric. The simulation model employed an available constitutive model, namely *MAT_249 in the commercial finite element software LS-DYNA. This constitutive model captured the nonlinear anisotropic hyperelastic response of the defined fiber families (e.g., carbon fibers (CFs), supporting glass fibers (GFs), and stitching), as well as the elasto-plastic shear deformation response of the fabric, which was uncoupled to the fiber extensional deformation.

During the first study, biaxial tension tests were performed on cruciform fabric specimens with varying ratios of deformation rate along the orthogonal CF tow (longitudinal) and supporting GF yarn (transverse) directions, including ratios R = 0.5, 1, and 2. These experimental test results were initially reported in a previous study by the authors. Captured force-strain responses along the CF tow and GF yarn directions revealed a minor tension-tension deformation coupling for the range of deformations considered, despite the observed interactions between the stitching and the CF tows. This outcome is a result of the higher fiber content and fabric stiffness along the longitudinal direction, which tended to suppress coupled biaxial tension deformation. The predicted nonlinear longitudinal and transverse force-strain responses for all displacement ratios correlated well with the experimental data, with slight deviations for the latter at higher strains. This discrepancy may be in part due to the assumed uncoupled extensional deformation response for each fiber family in the material model. However, indirect coupling was enabled by identifying a third fiber family representing the stitching and due to the superposition of the distinct stiffnesses for each fiber family. The predicted strain contours at the specimen center also correlated well with the experimentally measured DIC strain values for all R ratios.

Table 2 Predicted average shear angle within 50 × 50 mm^2 ROI at center of multi-branch specimen captured at a diagonal displacement of 1 mm for indicated test cases

CF tow orientation	Sh2_B1 shear angle [°]	Sh8_B1 shear angle [°]	Sh1_B2 shear angle [°]	Sh1_B8 shear angle [°]	Sh1_B16 shear angle [°]
0°	1.0	1.0	-	-	-
-45°	-	-	5.5	9.75	12.0
+45°	-	-	5.0	6.5	9.0

Journal : **Large 12289** | Article No : **1757** | Pages : **14** | MS Code : **1757** | Dispatch : **14-5-2023**

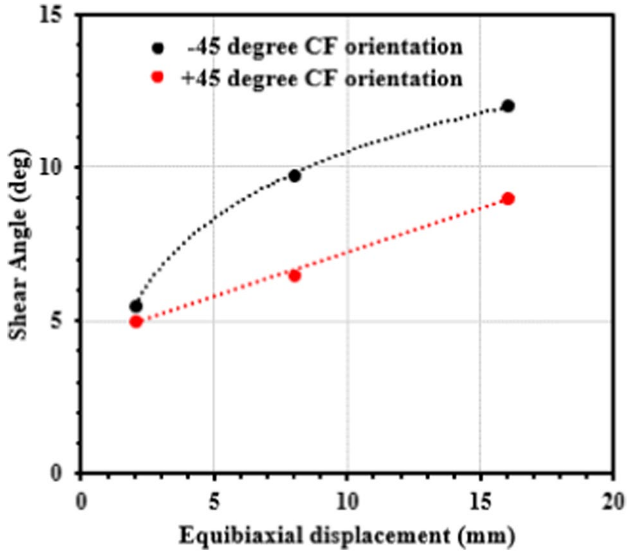

Fig. 11 Equibiaxial displacement-shear angle plots for simulated test cases from Table 2

For the next study, combined shear-equibiaxial tension tests were performed on specimens with three loading branches oriented along the longitudinal, transverse, and diagonal directions of the UD-NCF. The captured force-strain responses from tests with two different diagonal deformation rates revealed notable shear-extension coupling. However, due to the applied tension load along both the orthogonal CF tow and GF yarns, the extent of shear deformation at the specimen center was limited. The force-strain response predicted by the simulation model correlated very well with the experimental data, where for the latter engineering strains were determined from the displacements captured by the device displacements. These results demonstrated the capability of the model to capture the coupled shear-extension deformation response of the UD-NCF.

In the final study, the simulation model was used to predict shear angle at the center of the same multi-branch specimens for cases when the CF tow orientation was biased at +45° or -45° from the horizontal branch. The extent of shear deformation at the specimen center was notably greater for both cases when compared to the previous study owing to the fact that tensioning was only applied along either the CF tow or GF yarn direction. The main outcome of this final study was that the coupled shear-extension deformation of the UD-NCF is sensitive to the direction of tension loading.

One of the main contributions of this work is the proposed experimental setup for characterizing the coupled membrane deformation modes of reinforcement fabrics. The findings of the performed studies provide an improved understanding of the coupled biaxial tension and shear-biaxial tension deformations for UD-NCFs which were previously lacking in the literature. The notable coupling between the shear deformation and the longitudinal/transverse stiffness of the fabric is deemed necessary to be captured by material models used in macroscopic forming simulations. The presented results can also provide guidance for future studies focused on formability of UD-NCFs, in particular controlling pre-tensioning during forming operations to reduce the formation of shear-induced defects such as wrinkling and fiber waviness. Future work will be aimed at further investigating the effect of various magnitudes of pre-tensioning along the CF tow and GF yarn directions on the shear deformation of the UD-NCF over a larger range of deformations, as well as developing a material model that can directly capture the coupled membrane deformation modes in macroscopic forming simulations.

Acknowledgements The authors thank the Natural Sciences and Engineering Research Council of Canada (NSERC) for supporting this study through funding grant CRDPJ-507776-16, as well as the Advanced Manufacturing Consortium (AMC) of Ontario, Honda Development and Manufacturing of America LLC., Hexion Inc., Zoltek Corp., and Laval International for financial support. The Textiles HUB, laboratory at Politecnico di Milano, is gratefully acknowledged for access to the testing device.

Declarations

Conflict of interest The authors declare that they have no conflict of interest.

References

1. Ghazimoradi M, Trejo EA, Butcher C, Montesano J (2022) Characterizing the macroscopic response and local deformation mechanisms of a unidirectional non-crimp fabric. Compos Part A 156:106857. https://doi.org/10.1016/j.compositesa.2022.106857
2. Kärger L, Galkin S, Kunze E, Gude M, Schäfer B (2021) Prediction of forming effects in UD-NCF by macroscopic forming simulation – capabilities and limitations. 24th Int Conf Mater Form (ESAFORM 2021) Liege 14–16 April. https://doi.org/10.25518/esaform21.355
3. Schirmaier FJ, Dörr D, Henning F, Kärger L (2017) A macroscopic approach to simulate the forming behaviour of stitched unidirectional non-crimp fabrics (UD-NCF). Compos Part A 102:322–335. https://doi.org/10.1016/j.compositesa.2017.08.009
4. Carvelli V, Pazmino J, Lomov SV, Verpoest I (2012) Deformability of a non-crimp 3D orthogonal weave E-glass composite reinforcement. Compos Sci Technol 73:9–18. https://doi.org/10.1016/j.compscitech.2012.09.004
5. Ghazimoradi M, Carvelli V, Marchesi MC, Frassine R (2018) Mechanical characterization of tetraxial textiles. J Ind Text 48:3–24. https://doi.org/10.1177/1528083717721920
6. Komeili M, Milani AS. Response surfaces of mechanical behavior of dry woven fabrics under combined loadings. 19th International Conference on Composite Materials (ICCM19), Montreal, Canada, July 28 – Aug 2, 2013

Journal : Large 12289	Article No : 1757	Pages : 14	MS Code : 1757	Dispatch : 14-5-2023

7. Launay J, Hivet G, Duong AV, Boisse P (2008) Experimental analysis of the influence of tensions on in plane shear behaviour of woven composite reinforcements. Compos Sci Technol 68:506–515. https://doi.org/10.1016/j.compscitech.2007.06.021
8. Nosrat-Nezami F, Gereke T, Eberdt C, Cherif C (2014) Characterisation of the shear–tension coupling of carbon-fibre fabric under controlled membrane tensions for precise simulative predictions of industrial preforming processes. Compos Part A 67:131–139. https://doi.org/10.1016/j.compositesa.2014.08.030
9. Abdiwi F, Harrison P, Guo Z, Potluri P, Yu WR (2011) Measuring the shear-tension coupling of engineering fabrics. AIP Conf Proc 1353:889–894. https://doi.org/10.1063/1.3589628
10. Kashani MH, Rashidi A, Crawford BJ, Milani AS (2016) Analysis of a two-way tension-shear coupling in woven fabrics under combined loading tests: global to local transformation of non-orthogonal normalized forces and displacements. Compos Part A 88:272–285. https://doi.org/10.1016/j.compositesa.2016.06.004
11. Ghazimoradi M, Trejo EA, Carvelli V, Butcher C, Montesano J (2021) Deformation characteristics and formability of a tricot-stitched carbon fiber unidirectional non-crimp fabric. Compos Part A 145:106366. https://doi.org/10.1016/j.compositesa.2021.106366
12. Komeili M, Milani AS (2016) On effect of shear-tension coupling in forming simulation of woven fabric reinforcements. Compos Part B 99:17–29. https://doi.org/10.1016/j.compositesb.2016.05.004
13. Ghazimoradi M, Carvelli V, Naouar N, Boisse P (2019) Experimental measurements and numerical modelling of the mechanical behaviour of a glass plain weave composite reinforcement. J Reinf Plast Compos 39:49–59. https://doi.org/10.1177/0731684419868846
14. Boisse P, Hamila N, Guzman-Maldonado E, Madeo A, Hivet G, dell'Isola F (2017) The bias-extension test for the analysis of in-plane shear properties of textile composite reinforcements and prepregs: a review. Int J Mater Form 10:473–492. https://doi.org/10.1007/s12289-016-1294-7
15. Härtel F, Böhler P, Middendorf P (2014) An integral mesoscopic material characterization approach. Key Eng Mater 611–612:280–291. https://doi.org/10.4028/www.scientific.net/KEM.611-612.280
16. Schirmaier FJ, Weidenmann KA, Kärger L, Henning F (2016) Characterisation of the draping behaviour of unidirectional non-crimp fabrics (UD-NCF). Compos Part A 80:28–38. https://doi.org/10.1016/j.compositesa.2015.10.004
17. Krogh C, Kepler JA, Jakobsen J (2021) Pure and simple: investigating the in-plane shear kinematics of a quasi-unidirectional glass fiber non-crimp fabric using the bias-extension test. Int J Mater Form 14:1483–1495. https://doi.org/10.1007/s12289-021-01642-8
18. Trejo EA, Ghazimoradi M, Butcher C, Montesano J (2020) Assessing strain fields in unbalanced unidirectional non-crimp fabrics. Compos Part A 130:105758. https://doi.org/10.1016/j.compositesa.2019.105758
19. Naouar N, Hivet G, Vidal-Sallé E (2021) Mesoscopic approaches for composite reinforcement mechanical behavior. In: Boisse P (ed) Compos. Reinf. Optim. Perform. 2nd Ed. Woodhead Publishing, pp 499–536. https://doi.org/10.1016/B978-0-12-819005-0.00016-2
20. Harrison P (2012) Normalisation of biaxial bias extension test results considering shear tension coupling. Compos Part A 43:1546–1554. https://doi.org/10.1016/j.compositesa.2012.04.014
21. Potluri P, Ciurezu DAP, Young RJ. Biaxial shear testing of textile preforms for formability analysis. 16th International Conference on Composite Materials (ICCM16), Kyoto, Japan, July 8–13, 2007
22. Gereke T, Döbrich O, Hübner M, Cherif C (2013) Experimental and computational composite textile reinforcement forming: a review. Compos Part A 46:1–10. https://doi.org/10.1016/j.compositesa.2012.10.004
23. Pazmino J, Mathieu S, Carvelli V, Boisse P, Lomov SV (2015) Numerical modelling of forming of a non-crimp 3D orthogonal weave E-glass composite reinforcement. Compos Part A 72:207–218. https://doi.org/10.1016/j.compositesa.2015.02.013
24. Khan MA, Mabrouki T, Vidal-Sallé E, Boisse P (2010) Numerical and experimental analyses of woven composite reinforcement forming using a hypoelastic behaviour. Application to the double dome benchmark. J Mater Process Technol 210:378–388. https://doi.org/10.1016/j.jmatprotec.2009.09.027
25. Charmetant A, Orliac JG, Vidal-Sallé E, Boisse P (2012) Hyperelastic model for large deformation analyses of 3D interlock composite preforms. Compos Sci Technol 72:1352–1360. https://doi.org/10.1016/j.compscitech.2012.05.006
26. Peng XQ, Cao J (2005) A continuum mechanics-based non-orthogonal constitutive model for woven composite fabrics. Compos Part A 36:859–874. https://doi.org/10.1016/j.compositesa.2004.08.008
27. Döbrich O, Gereke T, Diestel O, Krzywinski S, Cherif C (2014) Decoupling the bending behavior and the membrane properties of finite shell elements for a correct description of the mechanical behavior of textiles with a laminate formulation. J Ind Text 44:70–84. https://doi.org/10.1177/1528083713477442
28. Aimène Y, Vidal-Sallé E, Hagège B, Sidoroff F, Boisse P (2010) A hyperelastic approach for composite reinforcement large deformation analysis. J Compos Mater 44:5–26. https://doi.org/10.1177/0021998309345348
29. Werner HO, Schäfer F, Henning F, Kärger L. Material modelling of fabric deformation in forming simulation of fiber-metal laminates – A review on modelling fabric coupling mechanisms. 24th International Conference on Material Forming (ESAFORM 2021), Liege, 14–16 April, 2021
30. Schäfer F, Werner HO, Henning F, Kärger L (2022) A hyperelastic material model considering biaxial coupling of tension-compression and shear for the forming simulation of woven fabrics. Compos Part A 165:107323. https://doi.org/10.1016/j.compositesa.2022.107323
31. Lee W, Cao J (2009) Numerical simulations on double-dome forming of woven composites using the coupled non-orthogonal constitutive model. Int J Mater Form 2(1):145–148. https://doi.org/10.1007/s12289-009-0499-4
32. Lee W, Byun J, Um M, Cao J, Boisse P. Couples non-orthogonal constitutive model for woven fabric composites. 17th International Conference on Composite Materials (ICCM17), Edinburgh, UK, 27–31 July, 2009
33. Yao Y, Huang X, Peng X, Liu P, Youkun G (2019) An anisotropic hyperelastic constitutive model for plain weave fabric considering biaxial tension coupling. Text Res J 89(3):434–444. https://doi.org/10.1177/0040517517748495
34. Yao Y, Peng X, Gong Y (2019) Influence of tension–shear coupling on draping of plain weave fabrics. J Mater Sci 54(8):6310–6322. https://doi.org/10.1007/s10853-019-03334-w
35. Schäfer B, Haas S, Boisse P, Kärger L (2022) Investigation of the membrane behavior of UD-NCF in Macroscopic Forming Simulations. Key Eng Mater 926:1413–1422. https://doi.org/10.4028/p-2977b4

36. Senner T, Kreissl S, Merklein M, Meinhardt J, Lipp A (2014) A modular modeling approach for describing the in-plane forming behavior of unidirectional non-crimp-fabrics. Prod Eng 8:635–643. https://doi.org/10.1007/s11740-014-0561-z
37. LS-DYNA User's Manual Volume II – Material Models. Livermore Software Technology Corporation (2020)
38. Ziegs J, Weck D, Gude M, Kastner M. Numerical modeling of single-step thermoforming of a hybrid metal/FRP lightweight structure. 18th European Conference on Composite, Materials (ECCM18), Athens, Greece, 24–28 June, 2018
39. Ghazimoradi M, Montesano J (2022) Macroscopic forming simulation for a unidirectional non-crimp fabric using an anisotropic hyperelastic material model. (under review)

Journal:	**12289**
Article:	**1757**

Author Query Form

Please ensure you fill out your response to the queries raised below and return this form along with your corrections

Dear Author

During the process of typesetting your article, the following queries have arisen. Please check your typeset proof carefully against the queries listed below and mark the necessary changes either directly on the proof/online grid or in the 'Author's response' area provided below

Query	Details Required	Author's Response
AQ1	Please check if the affiliations are presented correctly.	
AQ2	Please provide complete bibliographic details of this reference.	
AQ3	Please provide complete bibliographic details of this reference.	